Kinetics and Mechanism of the Multiple Addition Microemulsion Polymerization of Hexyl Methacrylate

Kevin D. Hermanson and Eric W. Kaler*

Center of Molecular Engineering and Thermodynamics, Department of Chemical Engineering, University of Delaware, Newark, Delaware 19716

Received October 25, 2002; Revised Manuscript Received January 6, 2003

ABSTRACT: Monomer can be added during the polymerization of a microemulsion in order to increase the amount of polymer produced. Here reported are the polymerization kinetics of a microemulsion of water, *n*-hexyl methacrylate (C_6MA), dodecyltrimethylammonium bromide (DTAB), and didodecyldimethylammonium bromide (DDAB) to which the monomer is added during polymerization. The kinetic model developed by Morgan and Kaler [*Macromolecules* **1997**, *30*, 1897−1905] is used to examine polymerization mechanisms and is extended to predict the evolution of particle size. The results show that radicals initiated prior to monomer addition do not polymerize the added monomer and that monomer partitioning, radical exit, and the number of active radicals initiated prior to an addition can limit final particle size. The small increase in average particle size after each monomer addition indicates that new particles are nucleated and grow in each step.

1. Introduction

Microemulsion polymerization conveniently produces nanoscale polymer latexes with high molecular weights ($\sim 1 \times 10^7$ Da).[1−14] Despite the many potential applications of such polymer latexes, commercial use of microemulsion polymerization processes has been limited because typical formulations are dilute in polymer and require a large ratio of surfactant to monomer. Surfactant concentrations usually exceed the amount required for polymer stability by factors as large as 20.

A number of studies have suggested that surfactant could be used more efficiently in microemulsion polymerization if the empty micelles in the final polymer dispersion were refilled with monomer and repolymerized to form a latex solution higher in polymer content but containing the original amount of surfactant.[15−21] Three variations of this method have been reported in the literature, viz. (i) a discontinuous polymerization method wherein the monomer was added at specified points during the reaction[16,21] (this is called multiple addition polymerization here), (ii) a continuous method wherein monomer was added continuously to the reacting system,[15,17,19] and (iii) a Winsor I method wherein the monomer was adsorbed into the micelles from an excess oil phase.[18,20] The final latex properties, most notably the particle size, depend considerably on the microemulsion and method used. In some cases the added monomer was mostly polymerized in preexisting particles so that there was a significant increase in particle size after each addition.[15−17,21] In other situations the particle size remained almost constant.[15] Factors proposed to affect the change in particle size include monomer solubility,[15,17,21] diffusion limitations,[17] and the amount of monomer.[15]

The Morgan−Kaler model and its extensions[8,11] provide a reliable and general description of microemulsion polymerization. Here this approach is extended and compared to the measured kinetics of a polymerizing microemulsion with monomer added discontinuously. The kinetic model is further extended to evaluate the evolution in particle size during polymerization, and comparison with data allows identification of key mechanistic steps. The polymerization system considered here consists of water and *n*-hexyl methacrylate (C_6MA) stabilized by a mixture of dodecyltrimethylammonioum bromide (DTAB) and didodecyldimethylammonium bromide (DDAB). The kinetics of this system have been studied extensively previously,[5−8,11] and because of the low glass transition temperature of poly-C_6MA and the linear partitioning of C_6MA between micelle and polymer, this mixture is nearly ideal for the study of microemulsion polymerization.[5−8,11] Evaluation of measured multiple addition data demonstrates that very little of the added monomer swells preexisting particles and polymerizes, so that the average particle size increases only slightly after many additions.

* To whom correspondence should be addressed: Tel (302) 831-3553; e-mail kaler@che.udel.edu.

2. Materials and Methods

C_6MA (99% pure) from Scientific Polymer Products was vacuum-distilled to remove inhibitor and stored below 0 °C for less than 2 weeks before use. DTAB and DDAB from TCI America with 98% purity and the initiator 2,2′-azobis[2-(2-imidazolin-2-yl)propane] dihydrochloride (VA-044) (Wako Pure Chemicals Industries, Ltd.), were used as received. Water was distilled, deionized, and degassed under a vacuum.

Reaction kinetics were measured using a Mettler RC1 reaction calorimeter that allowed for real time kinetic monitoring. The reaction calorimeter was equipped with an AP01 glass reactor and an anchor type stir bar. The contents were stirred at a constant speed of 200 rpm.

To start the reaction, the calorimeter containing the surfactant was sparged with ultrahigh-purity argon for 10 min to remove oxygen. The degassed water was injected into the reaction calorimeter and stirred to dissolve the surfactant. The reactor contents were heated to 40 °C whereupon the reaction calorimeter was calibrated. Argon-sparged C_6MA preheated to 40 °C was injected to form 746 g of microemulsion with a composition by weight percentage of 0.48/3.77/1.26/94.4 C_6MA/DTAB/DDAB/H_2O (1 g of water was reserved for initiator solution). After allowing the microemulsion 20 min to come to thermodynamic equilibrium, 1 g of an argon-sparged VA-044/H_2O initiator solution was injected to give an overall initiator composition of 1.47×10^{-4} M. The reaction had an induction

10.1021/ma0216223 CCC: $25.00
Published on Web 02/28/2003

time of less than 30 s, indicating that the oxygen concentration was very low. After the first batch of monomer was completely reacted, a 4 mL sample was collected with an argon-sparged syringe. The collected sample was weighed, and a second dose of sparged monomer (preheated to 40 °C) was added to the reactor to give a C_6MA/H_2O weight ratio of 0.005. The induction time of the added monomer was less than 30 s, indicating that a low oxygen environment was maintained. These processes were repeated, and after the complete reaction of each monomer addition, the latex was once again sampled and more monomer was added at the same C_6MA/H_2O ratio. The final conversions of the sampled latexes were measured to be greater than 99% using gravimetry. The processes continued until a final latex content of 17.1% was achieved, which required 43 separate additions.

Quasi-elastic light scattering (QLS) measurements were made at a constant temperature of 25 °C with an Ar^+ ion laser operating at a wavelength of 488 nm. The samples were diluted with a 0.73/0.24/99.02 DTAB/DDAB/H_2O micellar solution until the diameters measured by QLS no longer changed with dilution (at about 0.028 wt % polymer) and were filtered with 0.2 μm Whatman Anotop membrane filters. Mean hydrodynamic diameters were determined by assuming a single-exponential decay of the correlation function and subsequent use of the Stokes−Einstein relationship. The data were also analyzed by the CONTIN algorithm to determine any polydispersity in the size distribution.[22,23]

3. Theory

In microemulsion polymerization an initiator (typically water-soluble) is added to a one-phase thermodynamically stable microemulsion containing monomer-swollen micelles. The initiator begins to propagate first in the water phase with the sparingly soluble monomer. Once the oligomeric chain reaches a critical degree of polymerization, the chain becomes amphiphilic enough to enter a swollen micelle. Upon entering, the chain continues to grow by consuming the monomer inside the micelle while the consumed monomer is replenished by diffusion from the surrounding uninitiated micelles. Monomer diffusion through the aqueous phase is fast compared to the propagation rate, causing the concentration of monomer at the locus of polymerization to be determined by thermodynamics.

Termination of a growing chain can occur by either biradical termination or chain transfer. The small particle size in microemulsion polymerization means that a "zero-one" situation exists that precludes two radicals from inhabiting the same particle. In addition, because of the large number of micelles compared to polymer particles, entry of a second radical into a particle is rare. Thus, chain transfer is the dominant mechanism for radical termination with most radical transfer occurring to monomer. After radical transfer to monomer, the newly formed monomeric radical can exit if the monomer water solubility is high enough and thereby produce a dead polymer particle. This general mechanism of microemulsion polymerization has been illustrated previously in detail.[5−9,11,12]

3.1. Single Addition Batch Kinetics. Assuming radical entry occurs without propagation in the aqueous phase, the fundamental equation for the kinetics of microemulsion polymerization is

$$\frac{\partial f}{\partial t} = \frac{k_p C N^*}{M_0} \tag{1}$$

where f is the fractional conversion of the total amount of monomer added, k_p is the polymer propagation rate constant, C is the monomer concentration at the locus of polymerization, M_0 is the total amount of monomer added in moles per liter of microemulsion, and N^* is the concentration of growing radicals.

To evaluate the right-hand side of eq 1, both N^* and C must be expressed in terms of conversion and known constants. N^* can be evaluated given that the rate of radical production in the aqueous phase, ρ_0, is

$$\rho_0 = 2k_d[I] \tag{2}$$

where [I] is the concentration of initiator in moles per liter of microemulsion. Neglecting biradical termination inside the particles and chain transfer to nonreacting species, the time rate of change of the number of radicals is

$$\frac{\partial N^*}{\partial t} = \rho \tag{3}$$

with $\rho = \gamma_{eff}\rho_0$, where γ_{eff} is a radical efficiency constant that accounts for termination in the aqueous phase (see section 4.1). N^* is then equal to ρt.

C can be related to the initial monomer concentration in the particles, C_0, by assuming that the monomer concentration in the particles varies linearly with the total polymer conversion, so

$$C = C_0(1 - f) \tag{4}$$

This relationship is thermodynamically determined and describes C well for similar $C_6MA/DTAB/DDAB/H_2O$ reacting microemulsions as shown by small-angle neutron scattering measurements.[5−8,11]

Combining eqs 1, 3, and 4 allows calculation of the conversion in terms of known constants as

$$\frac{\partial f}{\partial t} = \frac{k_p C_0 \rho}{M_0}(1 - f)t \tag{5}$$

Assuming ρ is constant over the life of the reaction gives by integration

$$f(t) = 1 - \exp\left(-\frac{k_p C_0}{M_0}\frac{\rho}{2}t^2\right) \tag{6}$$

3.2. Multiple Addition Kinetics. The fundamental rate equation can be easily integrated in the case of batch polymerizations. However, in cases where monomer is added during polymerization, C_0 and M_0 are functions of time, and more importantly, C may not be completely determined by thermodynamics but may also be affected by the rate of monomer adsorption. For example, for the experimental system used here, agitation rates less than the used rate of 200 rpm were observed to have a major impact on reaction kinetics. At rates above 200 rpm, the agitation rate had a negligible effect on the measured reaction rate, indicating that monomer adsorption was fast compared to the reaction rate. Therefore, at high agitation rates the concentration of monomer at the locus of polymerization is assumed to be at thermodynamic equilibrium, so again

$$C = C_0(1 - f) \tag{7}$$

Unlike single addition batch polymerizations, multiple addition polymerizations can last for hours if there are a large number of additions. In this case the total

polymerization time may not be short compared to the initiator half-life, so ρ also cannot be approximated as constant. However, the rate of initiator decomposition is slow compared to the time between additions, so ρ is approximately constant for each interval. In this case, after the nth addition occurring at time t_n, N^* can be approximated as

$$N^* = \rho_n(t - t_n) + \sum_{k=1}^{n-1} \rho_k(t_{k+1} - t_k) \tag{8}$$

where

$$\rho_i = \gamma_{\text{eff}} 2k_{\text{d}}[\text{I}]^0 \exp(-k_{\text{d}} t_i) \tag{9}$$

and subscripts n and k denote the conditions at the start of addition number n and k. The two terms in eq 8, $\rho_n(t - t_n)$ and $\sum_{k=1}^{n-1}\rho_k(t_{k+1} - t_k)$, respectively represent the number of radicals produced during the polymerization of addition n and the number of radicals formed prior to addition n.

Because monomer is added discontinuously during multiple addition polymerizations, the fundamental rate equation can be solved for the times between monomer additions. Solving eq 1 for addition number n by substitution of eq 8 gives

$$f = 1 - (1 - f_n)\exp\left(-\frac{k_{\text{p}}C_{0,n}}{M_{0,n}}\left(\frac{\rho_n}{2}(t - t_n)^2 + \sum_{k=1}^{n-1}\rho_k(t_{k+1} - t_k)(t - t_n)\right)\right) \tag{10}$$

The only variable on the right-hand side of eq 10 that is not a constant for each reaction is time, t. In this expression f is the fractional conversion of total monomer added in n number of additions, $M_{0,n}$ is the total amount of monomer added through n additions, and subscripts denote conditions immediately following the nth addition, except for $C_{0,n}$ which represents the theoretical monomer concentration at the locus of polymerization for a system with a monomer concentration equal to $M_{0,n}$ and $f = 0$.

Equation 10 relates the fractional conversion of monomer added in n additions to the total amount of added monomer. It is more useful to relate the conversion of monomer added in each addition, $f_{b,n}$, to the amount of monomer added in each addition, $M_{0,b,n}$, if the reaction is allowed to proceed to near completion after each addition (that is, $f_{b,n} \rightarrow 1$). Equation 10 can be transformed using $f = (M_{0,n} - M_{0,b,n}(1 - f_{b,n}))/M_{0,n}$, $f_n = (M_{0,n} - M_{0,b,n})/M_{0,n}$, and the new variable $C_{0,b,n} = C_{0,n}(1 - f_n)$. $C_{0,b,n}$ represents the monomer concentration at the locus of polymerization immediately following the nth addition. With these transformations the kinetic equation becomes

$$f_{b,n} = 1 - \exp\left(-\beta_n\left(\frac{\rho_n}{2}(t - t_n)^2 + \sum_{k=1}^{n-1}\rho_k(t_{k+1} - t_k)(t - t_n)\right)\right) \tag{11}$$

where

$$\beta_n = \frac{k_{\text{p}}C_{0,b,n}}{M_{0,b,n}} \tag{12}$$

Because it is not at all certain that all radicals initiated prior to a given monomer addition, n, which is $\sum_{k=1}^{n-1}\rho_k(t_{k+1} - t_k)$, will participate in the polymerization of added monomer, the number of active surviving radicals can be represented more generally by N_n^{*0}, so that

$$f_{b,n} = 1 - \exp\left(-\beta_n\left(\frac{\rho_n}{2}(t - t_n)^2 + N_n^{*0}(t - t_n)\right)\right) \tag{13}$$

Note that the same result is obtained if each addition is viewed as an independent reaction starting at time t_n with $N^* = \rho_n(t - t_n) + N_n^{*0}$ and $C = C_{0,b,n}(1 - f_{b,n})$. In this case

$$\frac{\partial f_{b,n}}{\partial t} = \frac{k_{\text{p}}C_{0,b,n}}{M_{0,n}}(1 - f_{b,n})(\rho_n(t - t_n) + N_n^{*0}) \tag{14}$$

and integration yields eq 13.

4. Results and Discussion

4.1. Multiple Addition Kinetics. The Morgan–Kaler model accurately predicts the polymerization kinetics of a single batch of C_6MA/DTAB/DDAB/H_2O microemulsion.[5–8,11] Here we compare the measured and predicted results for a multiple addition polymerization. Because all of the constants on the right-hand side of eq 14, with the exception of N_n^{*0}, can be evaluated from independent measurements, the measured reaction kinetics can be used to determine whether radicals initiated prior to a monomer addition are fed by the added monomer.

Figures 1 and 2 compare the reaction kinetics of the first four additions to the predicted reaction kinetics. The propagation rate constant was approximated to be $k_{\text{p}} = 680\ \text{M}^{-1}\ \text{s}^{-1}$ by interpolating pulsed-laser polymerization data for other linear alkyl methacrylates.[24] The dissociation rate constant of VA-044 was used as supplied by the manufacturer, $k_{\text{d}} = 1.1 \times 10^{-5}\ \text{s}^{-1}$, and the radical efficiency constant, γ_{eff}, was assumed to be 1.0. The monomer concentration in the microemulsion was determined by the composition of the system to be $M_{0,b,n} = 0.0297$ M, and the monomer concentration at the locus of polymerization, $C_{0,b,n}$, was determined from independently measured kinetic data of related single addition polymerization reactions to be 0.66, 0.56, 0.47, and 0.37 M for the first four additions, respectively, as discussed below. For each system the monomer concentration in the polymer particles, $C_{0,b,n}$, is much larger than the monomer concentration in the microemulsion, $M_{0,b,n}$, because monomer is restricted to the micelles and polymer. In other words, monomer is restricted to a volume smaller than the full microemulsion volume.

These values of $C_{0,b,n}$ were found by realizing that the composition at any stage of a multiple addition polymerization can be related to an equivalent single stage polymerization as follows. Consider the composition of the reaction mixture at the beginning of the second addition. The amount of unpolymerized monomer was $M_{0,b,n} = 0.0297$ M, and the amount of polymerized monomer was 0.0297 M. This composition was identical to a single addition polymerization with the same surfactant concentration and a starting monomer con-

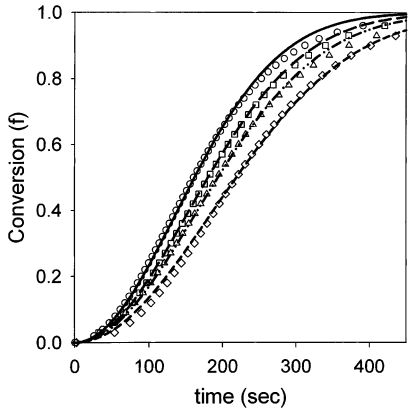

Figure 1. Comparison of the experimental (open symbols) and the predicted reaction kinetics (lines) using $N_n^{*0} = 0$: ○, first addition; □, second addition; △, third addition; ◇, fourth addition.

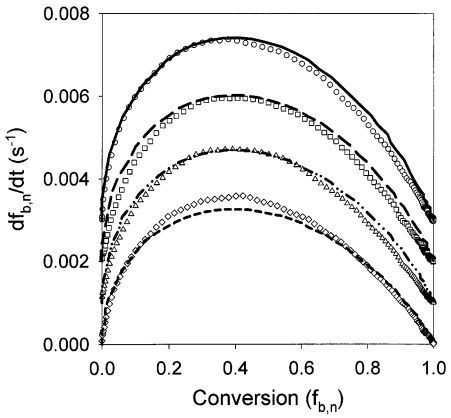

Figure 2. Comparison of the experimental curves (open symbols) and the predicted reaction rate (lines) using $N_n^{*0} = 0$. Curves are offset to show the model fit. ○, first addition (offset 0.003 s^{-1}); □, second addition (offset 0.002 s^{-1}); △, third addition (offset 0.001 s^{-1}); ◇, fourth addition.

centration of $M_0 = 0.0594$ M at a conversion, f, of 50%. This is a useful observation, because it means that by measuring the kinetics of a batch polymerization system with a monomer concentration of 0.0594 M and assuming linear monomer partitioning, $C_{0,b,2}$ can be determined independently for the second addition. Similarly, by measuring the single addition kinetics of microemulsions with initial C_6MA concentrations of 0.0891 and 0.1188 M, $C_{0,b,n}$ can be determined for the third and fourth additions. This approach means that in general the $C_{0,b,n}$ of any addition can be related to the C of a single addition situation with $M_0 = \sum_{k=1}^{n} M_{0,b,k}$ and $f = (M_0 - M_{0,b,n}(1 - f_{b,n}))/M_0$. This method will fail, however, when the required initial monomer concentration in the single addition case, M_0, is so high that a one-phase microemulsion does not form. In the case here, $C_{0,b,n}$ cannot be measured for additions beyond the fourth because the phase boundary is exceeded at monomer concentrations above 0.119 M.

Because C_0 is part of a group of constants in eq 5 it cannot be determined from single addition kinetic measurements without knowing the values of the other parameters. As long as N_n^{*0} varies as $\sum_{k=1}^{n-1} \rho_k (t_{k+1} - t_k)$, $C_{0,b,n}$ is also part of the same group of constants in eq 14. This means that by scaling the kinetics of a single addition reaction with the same initiator concentration by $(1 - f_{b,n})M_0/(1 - f)M_{0,n}$, the kinetics of a multiple addition reaction can be predicted. This situation negates the need for independent knowledge of k_p, k_d, and γ_{eff}, and the resulting kinetic predictions would be identical to those predictions made in Figure 3 by scaling C_0 to $C_{0,b,n}$ alone.

Figure 3a shows the measured kinetics and model fits for the single addition polymerizations used to determine $C_{0,b,n}$. The maximum rates measured occur at a conversion of 0.34 for the $M_0 = 0.0297$ M sample and 0.38 for the other three samples. These measured conversions agree reasonably well with the model predicted conversions of 0.39, indicating the assumption of linear monomer partitioning is valid.[5,6,8,11] The monomer partitioning data resulting from the model fits can be arranged into a monomer partitioning map that describes the concentration of monomer at the locus of polymerization for any system with the same surfactant concentration and a total monomer/polymer concentration less than 0.189 M (Figure 3b). Because the second addition of the multiple addition polymerization studied starts at a composition identical to a 50% conversion batch polymerization initially at 0.0594 M monomer, the monomer concentration at the locus of polymerization, C, during the polymerization of the second addition can be traced on the monomer partitioning map (Figure 3c). Likewise, the composition path followed during the polymerization of the third and fourth additions can also be traced on the partitioning map. By expressing the map in terms of the conversion of each addition, $f_{b,n}$, it is apparent that $C_{0,b,n}$ decreases for each of the first four monomer additions (Figure 3d). A consequence of this decrease is that the observed polymerization rate of each addition is slower than that of the preceding addition (Figure 4).

It is interesting that the kinetic model matched the measured data only with $N_n^{*0} = 0$, that is, when no radicals initiated in prior additions contribute to the kinetics of the current addition (Figures 1 and 2). The inactivity of prior initiated radicals is likely caused by either termination or by starvation of the active polymer chains for monomer. Although complete termination cannot be achieved through biradical termination,[25] preexisting radicals can be terminated by chain transfer to a nonreacting species. Many common surfactants as well as impurities can act as chain transfer agents.[26,27]

The active polymer chains could also be starved for monomer because of the slow diffusion of monomer in the polymer particles. Monomer diffusion coefficients in a polymer matrix higher than 90 wt % polymer are typically at least 2 orders of magnitude lower than those in solution.[28] If intraparticle monomer diffusion limitations exist, the majority of monomers will reside in the micelles and in the surfactant-rich shell coating the polymer particles. Such a nonequilibrium thermodynamic state is not inconsistent with the kinetic model developed here because the ultimate thermodynamically determined monomer partitioning occurs mostly between the swollen micelles and the aliphatic tails of surfactant surrounding the polymer.[5]

Although the values of $C_{0,b,n}$ cannot be predicted for additions above the fourth, the reaction rates for these subsequent additions can of course be measured. At higher additions the reaction rates continue to decrease asymptotically while the maximum rate occurs at lower conversions (Figures 5 and 6). Fitting the kinetic model to determine $C_{0,b,n}$ for each addition (again with $N_n^{*0} = 0$) shows that $C_{0,b,n}$ decreases to approximately 0.54 M (Figure 7).

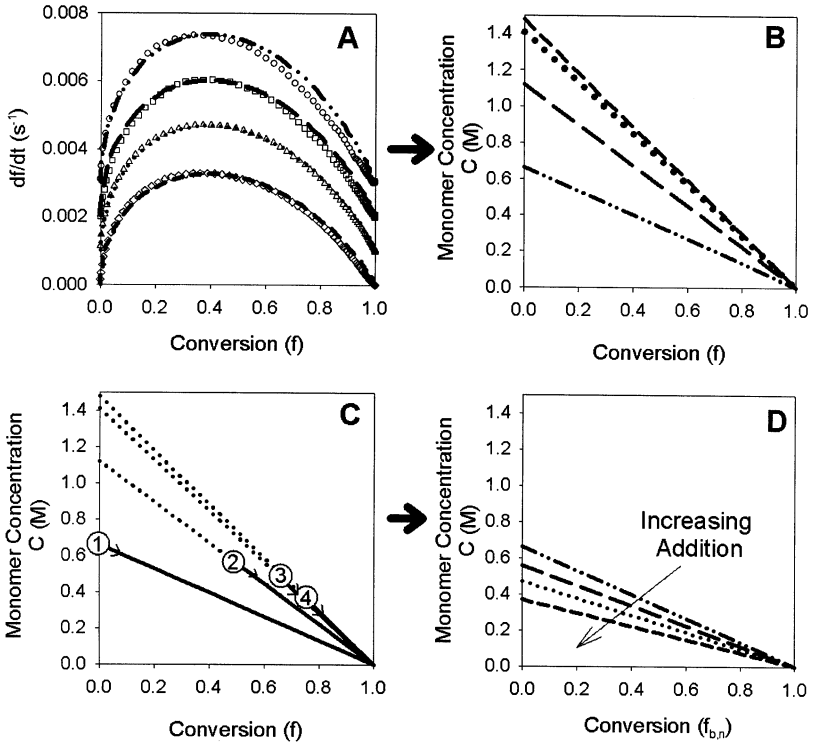

Figure 3. Calculation of monomer concentration at the locus of polymerization from experimental data assuming $\gamma_{eff} = 1.0$. (A) Measured single addition data (open symbols) and model fits (lines). (B) Monomer partitioning map on a total monomer added basis. (C) Polymerization path of multiaddition polymerization. (D) Monomer partitioning map on a monomer per addition basis. For graphs A and B: (−••−) $M_0 = 0.0297$ M, (− −) $M_0 = 0.0594$ M, (•••) $M_0 = 0.0891$ M, and (− − −) $M_0 = 0.1188$ M. See text for explanation.

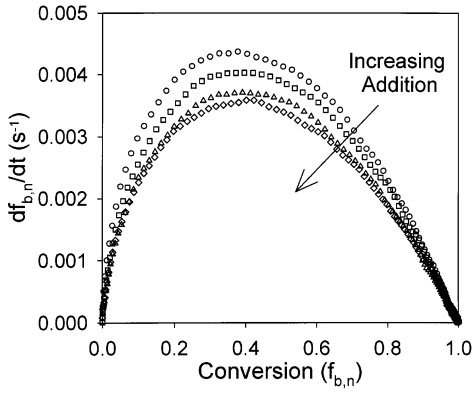

Figure 4. Rate vs conversion of monomer added in each batch for the multiaddition microemulsion polymerization of a C_6MA/DTAB/DDAB/H_2O microemulsion with VA-044 initiator: ○, first addition; □, second addition; △, third addition; ◇, fourth addition. $M_{0,b,n} = 0.0297$ M.

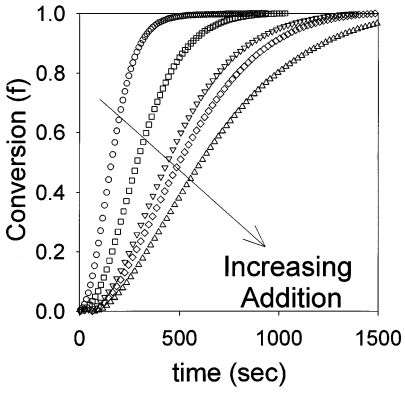

Figure 5. Reaction kinetics for each batch of the multiaddition microemulsion polymerization: ○, 1st addition; □, 11th addition; ▽, 21st addition; ◇, 31st addition; △, 41st addition. $M_{0,b,n} = 0.0296$ M.

4.2. Particle Size Evolution. QLS measurements show only a modest increase in particle diameter from 37.9 to 53.6 nm over the course of 43 additions (Figure 8). Thus, most of the added monomer formed new particles with the increase in particle size accounting for only 6.5% of the volume of added monomer. Had all of the monomer added to the first-generation particles, the final particles would be 130 nm in diameter (Figure 8). CONTIN analysis on a volume basis of the QLS measurements shows only a slight change in the particle size distribution (Figure 9).

To better understand the mechanisms leading to this limited growth, the reaction model derived previously was extended to describe the particle size evolution (Supporting Information). The model can be used to clarify why, if preexisting radicals are not active, a small amount of growth still occurred and what effects active radicals may have on particle growth.

An important factor in attaining any particle growth is whether radicals exit the formed particles, and in fact in the single batch case the particle size distributions are consistent with the exit of radicals.[12] The parameters used in the particle size analysis are the same as the parameters used for the kinetic analysis with the exception of the radical efficiency, γ_{eff}, and monomer concentration at the locus of polymerization, $C_{0,b,n}$.

As discussed earlier, because of the method used for the determination $C_{0,b,n}$, the numerical value of the radical efficiency used in the kinetic analysis does not affect the predictions of the kinetic model. However, the particle size predictions are sensitive to the radical efficiency, with larger radical efficiencies leading to predictions of smaller particles. For this portion of the

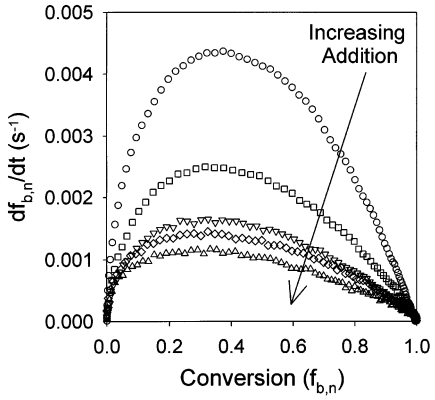

Figure 6. Rate vs conversion of monomer added in each batch for the multiaddition microemulsion polymerization of a C_6MA/DTAB/DDAB/H_2O microemulsion with VA-044 initiator: ○, 1st addition; □, 11th addition; ▽, 21st addition; ◇, 31st addition; △, 41st addition. $M_{0,b,n} = 0.0296$ M.

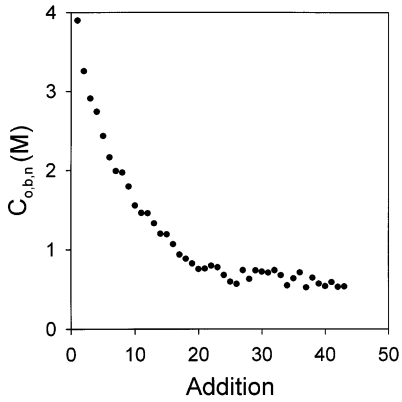

Figure 7. Calculated monomer concentration at the locus of polymerization assuming $N_n^{*0} = 0$ and $\gamma_{eff} = 0.17$ for all 43 additions.

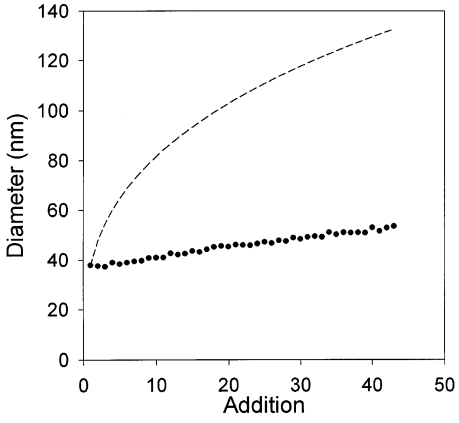

Figure 8. Particle sizes after each stage of multiaddition polymerization: (●) QLS measured particle size; (– – –) calculation of particle growth assuming no nucleation of new particles (see text).

analysis a radical efficiency of 0.17 was determined by matching the particle size predicted by the model for the first addition in the case of complete radical exit to the particle size measured by QLS (Figures 8 and 10). The $C_{0,b,n}$ values obtained from the single addition measurements using a 0.17 radical efficiency were also used in the particle size predictions. The time of monomer addition, t_k, was the experimental addition time and the chain transfer rate was set at a value similar to those for other alkyl methacrylates, $k_{tr} = 0.01$ M^{-1} s^{-1}.[12,29]

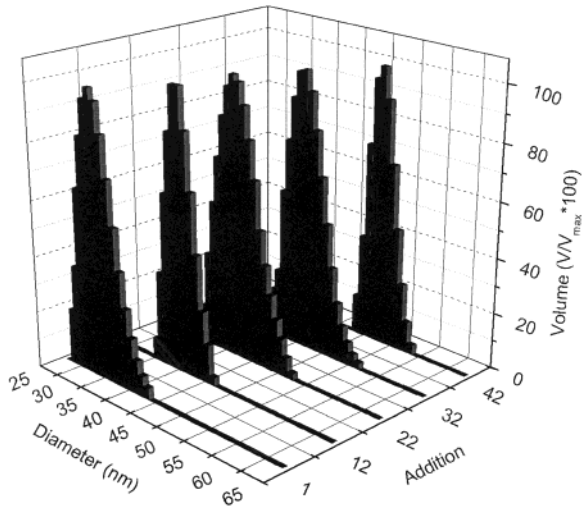

Figure 9. CONTIN analysis of particle size distribution for the multiaddition polymerization.

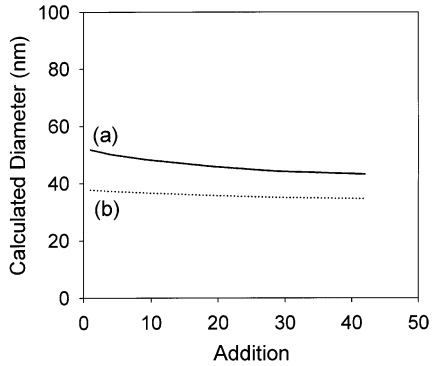

Figure 10. Model calculations of particle growth with no radicals active from previous additions: (a) —, with no radical exit; (b) ···, with radical exit. $M_{0,b,n} = 0.0296$ M, $k_p = 680$ M^{-1} s^{-1}, $k_d = 1.1 \times 10^{-5}$ s^{-1}, $\gamma_{eff} = 0.17$.

With these considerations, the only variable that changes between additions is the monomer concentration at the locus of polymerization, $C_{0,b,n}$. Using the adjusted $C_{0,b,n}$ values, the model predicts that the particle size would *decrease* slightly from 38 to 35 nm in the case with radical exit and from 52 to 43 nm in the case with no radical exit (Figure 10). This decrease results from a slower rate of propagation in each addition, and a resultant increase in the total number of particles initiated before monomer was exhausted. Under the model assumptions, if no preexisting radicals are fed by added monomer, the measured growth can only occur if the newly formed particles are larger than the preexisting particles. This does not occur when $C_{0,b,n}$ decreases with each addition. Further analyses of the effect of active preexisting radicals on particle growth are discussed in the Supporting Information.

Thus, the small increase in size observed experimentally in the C_6MA polymerization arises either from an undetectable contribution from preexisting radicals or from effects not considered in the particle growth model, most notably particle flocculation or radical reentry. No noticeable flocculation occurred in the latex over the 3 months following polymerization. However, radical reentry can occur because, unlike in single addition batch polymerizations[9] where the ratio of microemulsion droplets to latex particles is ~1000, in multiple addition polymerization the concentration of latex is ultimately an order of magnitude higher, so the micelle-to-particle

ratio is about 100. In this case approximately 1% of the new radicals will enter into existing particles and cause them to grow. The resulting growth will consume ~1% of added monomer, which is of the same order of magnitude as the measured consumption.

5. Conclusion

Experimental and theoretical results show that particle growth during multiple addition polymerizations can be influenced by monomer concentration at the locus of polymerization and the activity of radicals initiated prior to an addition. Reaction rate analysis for a DTAB/DDAB/C_6MA polymerization shows that monomer added to the polymerization does not react with radicals initiated prior to monomer addition. This is likely due either to diffusion limitations within the preexisting particles or to termination of preexisting radicals by chain transfer to surfactant. Particle sizes grow only modestly during the process, indicating that monomer polymerized in newly formed particles. Model predictions of particle size show that significant growth of preexisting particles containing active radicals can only be achieved in systems with low radical exit rates and a low radical efficiency (i.e., those producing a limited number of radicals). The results can be used to help control latex properties by the selection of reaction conditions for economical microemulsion polymerizations.

Supporting Information Available: The model predicted particle size evolution in a polymerization where the preexisting radicals remain active and an explanation of the particle size evolution model. This material is available free of charge via the Internet at http://pubs.acs.org.

References and Notes

(1) Candau, F.; Leong, Y. S.; Fitch, R. M. *J. Polym. Sci., Part A: Polym. Chem.* **1985**, *23*, 193−214.
(2) Candau, F. In *Polymerization in Organized Media*; Paleos, C. M., Ed.; Gordon and Breach Science Publishers: Philadelphia, PA, 1992; pp 215−282.
(3) Antonietti, M.; Bremser, W.; Muschenborn, D.; Rosenauer, C.; Schupp, B.; Schmidt, M. *Macromolecules* **1991**, *24*, 6636−6643.
(4) Antonietti, M.; Basten, R.; Lohmann, S. *Macromol. Chem. Phys.* **1995**, *196*, 441−466.
(5) Co, C. C.; Kaler, E. W. *Macromolecules* **1998**, *31*, 3203−3210.
(6) Co, C. C.; de Vries, R.; Kaler, E. W. *Macromolecules* **2001**, *34*, 3224−3232.
(7) Co, C. C.; Cotts, P.; Burauer, S.; de Vries, R.; Kaler, E. W. *Macromolecules* **2001**, *34*, 3245−3254.
(8) de Vries, R.; Co, C. C.; Kaler, E. W. *Macromolecules* **2001**, *34*, 3233−3244.
(9) Full, A. P.; Kaler, E. W.; Arellano, J.; Puig, J. E. *Macromolecules* **1996**, *29*, 2764−2775.
(10) Guo, J. S.; El-Aasser, M. S.; Vanderhoff, J. W. *J. Polym. Sci., Part A: Polym. Chem.* **1989**, *27*, 691−710.
(11) Morgan, J. D.; Lusvardi, K. M.; Kaler, E. W. *Macromolecules* **1997**, *30*, 1897−1905.
(12) Morgan, J. D.; Kaler, E. W. *Macromolecules* **1998**, *31*, 3197−3202.
(13) Guo, J. S.; Sudol, E. D.; Vanderhoff, J. W.; El-Aasser, M. S. *J. Polym. Sci., Part A: Polym. Chem.* **1992**, *30*, 703−712.
(14) Gan, L. M.; Chew, C. H.; Ng, S. C.; Loh, S. E. *Langmuir* **1993**, *9*, 2799−2803.
(15) Ming, W.; Jones, F. N.; Fu, S. K. *Macromol. Chem. Phys.* **1998**, *199*, 1075−1079.
(16) Rabelero, M.; Zacarias, M.; Mendizabal, E.; Puig, J. E.; Dominguez, J. M.; Katime, I. *Polym. Bull. (Berlin)* **1997**, *38*, 695−700.
(17) Ming, W. H.; Jones, F. N.; Fu, S. K. *Polym. Bull. (Berlin)* **1998**, *40*, 749−756.
(18) Gan, L. M.; Lian, N.; Chew, C. H.; Li, G. Z. *Langmuir* **1994**, *10*, 2197−2201.
(19) Xu, X. J.; Chew, C. H.; Siow, K. S.; Wong, M. K.; Gan, L. M. *Langmuir* **1999**, *15*, 8067−8071.
(20) Loh, S. E.; Gan, L. M.; Chew, C. H.; Ng, S. C. *J. Macromol. Sci., Pure Appl. Chem.* **1996**, *A33*, 371−384.
(21) Sosa, N.; Peralta, R. D.; Lopez, R. G.; Ramos, L. F.; Katime, I.; Cesteros, C.; Mendizabal, E.; Puig, J. E. *Polymer* **2001**, *42*, 6923−6928.
(22) Provencher, S. W. *Comput. Phys. Commun.* **1982**, *27*, 213−227.
(23) Provencher, S. W. *Comput. Phys. Commun.* **1982**, *27*, 229−242.
(24) Beuermann, S.; Buback, M.; Davis, T. P.; Gilbert, R. G.; Hutchinson, R. A.; Olaj, O. F.; Russell, G. T.; Schweer, J.; vanHerk, A. M. *Macromol. Chem. Phys.* **1997**, *198*, 1545−1560.
(25) Gilbert, R. G. *Emulsion Polymerization: A Mechanistic Approach*; Academic Press: San Diego, CA, 1995.
(26) Hunkeler, D.; Hamielec, A. E.; Baade, W. *Polymer* **1989**, *30*, 127−142.
(27) Hagiopol, C.; Deleanu, T.; Memetea, T. *J. Appl. Polym. Sci.* **1989**, *37*, 947−959.
(28) Griffiths, M. C.; Strauch, J.; Monteiro, M. J.; Gilbert, R. G. *Macromolecules* **1998**, *31*, 7835−7844.
(29) *Polymer Handbook*, 3rd ed.; John Wiley & Sons: New York, 1989.
(30) Finsy, R.; Dejaeger, N. *Part. Part. Syst. Charact.* **1991**, *8*, 187−193.

MA0216223